



ELSEVIER

Available online at www.sciencedirect.com



Information Processing Letters ●●● (●●●) ●●●-●●●

Information
Processing
Letters

www.elsevier.com/locate/ipl

Voronoi diagrams of moving points in the plane and of lines in space: tight bounds for simple configurations

Amit Weisman^a, L. Paul Chew^b, Klara Kedem^{a,b,*}^a Department of Computer Science, Ben Gurion University, Be'er Sheva, Israel^b Computer Science Department, Cornell University, Ithaca, NY, USA

Received 27 November 2003; received in revised form 8 April 2004

Communicated by F. Dehne

Abstract

The combinatorial complexities of (1) the Voronoi diagram of moving points in 2D and (2) the Voronoi diagram of lines in 3D, both under the Euclidean metric, continues to challenge geometers because of the open gap between the $\Omega(n^2)$ lower bound and the $O(n^{3+\epsilon})$ upper bound. Each of these two combinatorial problems has a closely related problem involving Minkowski sums: (1') the complexity of a Minkowski sum of a planar disk with a set of lines in 3D and (2') the complexity of a Minkowski sum of a sphere with a set of lines in 3D. These Minkowski sums can be considered “cross-sections” of the corresponding Voronoi diagrams. Of the four complexity problems mentioned, problems (1') and (2') have recently been shown to have a nearly tight bound: both complexities are $O(n^{2+\epsilon})$ with lower bound $\Omega(n^2)$.

In this paper, we determine the combinatorial complexities of these four problems for some very simple input configurations. In particular, we study point configurations with just two *degrees of freedom* (DOF), exploring both the Voronoi diagrams and the corresponding Minkowski sums. We consider the traditional versions of these problems to have 4 DOF. We show that even for these simple configurations the combinatorial complexities have upper bounds of either $O(n^2)$ or $O(n^{2+\epsilon})$ and lower bounds of $\Omega(n^2)$.

© 2004 Published by Elsevier B.V.

Keywords: Computational geometry; Combinatorial problems; Voronoi diagrams

1. Introduction

In this paper we present some very simple input configurations, which we call 2-DOF configurations,

and show that even for these configurations the combinatorial complexity of the Voronoi diagrams (and the Minkowski sums) are about $\Theta(n^2)$.

We explore aspects of four very well known and closely related problems in computational geometry: the combinatorial complexities of (1) the Voronoi diagram of moving points in the plane—each with its own

* Corresponding author.

E-mail address: klara@cs.bgu.ac.il (K. Kedem).

constant velocity—under the Euclidean metric, (2) the Voronoi diagram of lines in 3D under the Euclidean metric, (1') the boundary of the Minkowski sum of a disk with a set of lines in 3D, and (2') the boundary of the Minkowski sum of a sphere with a set lines in 3D. Problems (1) and (2) have a significant gap between their respective lower bounds ($\Omega(n^2)$) and their current best upper bounds ($O(n^{3+\epsilon})$) [6,10,2]. It is widely believed that, for problems (1) and (2), the true combinatorial complexity is close to quadratic, but despite great efforts by many geometers the gaps between lower and upper bounds remain. For problems (1') and (2'), almost tight bounds are now known ($\Omega(n^2)$ and $O(n^{2+\epsilon})$) [1]. The diagram in Fig. 1 illustrates the connections between the above mentioned problems and their simplifications.

1.1. The Voronoi diagram of moving points in the plane

Let P be a set of n points in the plane. Each point p_i has a constant velocity v_i assigned to it. At time $t = 0$ all points start moving. The combinatorial complexity of the Voronoi diagram of the moving points is the number of combinatorially distinct Voronoi edges

and vertices that appear as t advances from zero to infinity. A Voronoi edge is described by a pair $\{p, q\}$ of sites, and a Voronoi vertex is described by a triple of sites $\{p, q, r\}$. The best bound known for the combinatorial complexity of this problem is $O(n^{3+\epsilon})$ [6,10]. Tight bounds have been shown for two simplified versions of this problem.

- If the set P is divided into k subsets, each subset moving rigidly (i.e., every point within a subset shares the same velocity), then [7] showed a quadratic bound in n : $O(n^2 k^2 \lambda_2(k))$, where $\lambda_2(k)$ is almost linear in k .
- If the distance function is L_1 or L_∞ (or any polygon-based distance function) then the combinatorial complexity of the Voronoi diagram of moving points is $O(n^2 \alpha(n))$ [4].

1.2. The Voronoi diagram of lines in 3D

Let L be a set of n lines in 3D. Such a set of lines has a well-defined Voronoi diagram (i.e., each line has a Voronoi region consisting of all points closer to that line than to any other line) under the standard Euclidean metric; we are interested in the combina-

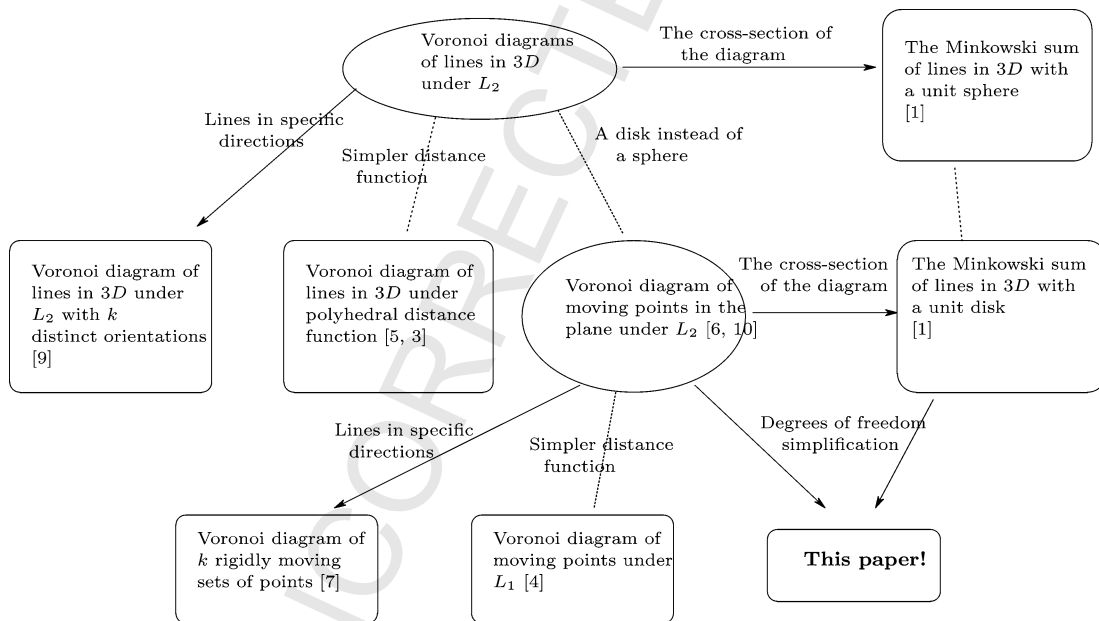


Fig. 1. Relations between problems. Solid lines denote subproblems; dotted lines denote parallel problems (e.g., using L_1 instead of the standard L_2 distance).

torial complexity of this Voronoi diagram (i.e., the number of Voronoi surfaces, edges, and vertices). It is trivial to show a lower bound of $\Omega(n^2)$. The best upper bound known is $O(n^{3+\varepsilon})$ [2]. For this problem also, tight bounds have been shown for simplified versions.

- If the set L of lines is divided into k subsets, each subset consisting of parallel lines, then the upper bound is $O(n^{2+\varepsilon})$ [9].
- If a polyhedral distance function is used instead of the standard Euclidean metric then the upper bound is $O(n^{2+\varepsilon})$ [3,5].

Notice that the simplified versions here are essentially the same as those for the Voronoi diagram of moving points.

1.3. The corresponding Minkowski sums

The combinatorial complexity of the Minkowski sum of a unit sphere (or a unit disc) with a set of lines in 3D is the number of surfaces, edges, and vertices on the sum's boundary. This boundary is essentially a *cross-section* of the corresponding Voronoi diagram (i.e., a cross-section at distance 1 from the lines). Intuitively, one hopes that the combinatorial complexity of the Minkowski sums serves as an indication of the complexity of the corresponding Voronoi diagram. Recently [1], these Minkowski sums have been shown to have complexities of $O(n^{2+\varepsilon})$ with lower bound $\Omega(n^2)$.

1.4. Degrees of freedom

In the traditional problem definition for the Voronoi diagram of moving points in the plane each point p has four *degrees of freedom* (DOF): (x_0, y_0, v_x, v_y) where (x_0, y_0) is the initial location of point p and (v_x, v_y) is its velocity vector. In this paper we consider the restricted input configuration where all the points are initially located on the x axis and have a velocity vector of $(0, v_y)$. At first glance, this problem looks far simpler than the original problem, each point having just two DOF $(x_0, 0, 0, v_y)$ rather than four. We show in this paper that despite the simplicity of the input configuration, the resulting Voronoi diagram has $\Theta(n^2)$ complexity. Note that by choosing different pairs, we

can define several additional 2 DOF problems; these are briefly discussed in Section 2.3.

2. Moving points in the plane with 2 DOF

Let $P = \{p_1, p_2, \dots, p_n\}$ be a set of points placed on the x axis at positions (x_1, x_2, \dots, x_n) , respectively. Each point has a constant velocity (v_1, v_2, \dots, v_n) , respectively, with a y axis component only. What is the combinatorial complexity of the resulting Voronoi diagram as t advances from zero to infinity?

Observe that the points remain in the same relative positions as time changes from $t = 1$ to $t = 2$. In other words, each point is exactly twice as far from the x axis at $t = 2$ as it is at $t = 1$. We can pretend that the points are in fixed position on a rubber sheet. The sheet is stretched in the y direction as time passes. Alternately, we can pretend that the points are in fixed position on a nonstretching plane, but the distance function changes from the standard Euclidean distance, based on a circle, (at $t = 1$) to one based on an ellipse (the ellipse is squashed in the y direction as time advances). The two views are exactly equivalent; squashing the distance function in the y direction is equivalent to stretching the distance function in the x direction, since for Voronoi diagrams we are interested only in relative distances.

2.1. Lower bound example

In this Subsection we construct an example that shows $\Omega(n^2)$ combinatorially distinct Voronoi edges, based on the observation that the Voronoi diagram for moving points in the plane under Euclidian distance is equivalent to the Voronoi diagram for fixed points under a changing ellipse-based distance function.

Claim 2.1. *Given a line L through the origin and of nonzero slope, and given a position x_0 on the x axis, there is a continuum of ellipses tangent to the x axis at x_0 and also tangent to L .*

The proof of this claim is straightforward. A picture is pretty convincing (see Fig. 2). If L forms an acute angle with the x axis, then the tangency points on L reside on a segment $\subset L$ starting at $y = 0$ and ending at the point Q where the circle (at time $t = 1$) is tangent

49
50
51
52
53
54
55
56
57
58
59
60
61
62
63
64
65
66
67
68
69
70
71
72
73
74
75
76
77
78
79
80
81
82
83
84
85
86
87
88
89
90
91
92
93
94
95
96

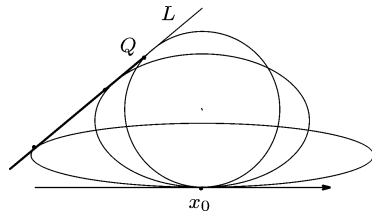


Fig. 2. Ellipses tangent to the horizontal line at point x_0 and to the diagonal line L .

to x axis at x_0 and to L at Q . Stopping at $t = 1$ is arbitrary, but is enough to show quadratic behaviour in the proof below.

Lemma 2.2. For n points in the plane, each starting on the x axis and each having its own constant velocity parallel to the y axis, the complexity of the resulting Voronoi diagram is $\Omega(n^2)$.

Proof. Place $n/2$ points $(p_1, p_2, \dots, p_{n/2})$ on the x axis; these points are assigned speed equal zero. Each point p_i has a segment $S_i \subset L$ assigned to it, all segments starting at $y = 0$. The rest of the points $(q_1, q_2, \dots, q_{n/2})$ are placed on the segment $\cap S_i$, which cannot be empty. By Claim 2.1 for any pair (p_i, q_j) there exists an ellipse tangent to the x axis at p_i and to L at q_j . Therefore there are $\Omega(n^2)$ such ellipses; further, by construction, each such ellipse is empty of any other point of P . Thus, each such ellipse is a witness for a distinct Voronoi edge between p_i and q_j . Hence there are $\Omega(n^2)$ Voronoi edges. \square

2.2. Upper bound

Theorem 2.3. Given a set of n moving points P satisfying our 2 DOF restrictions, and in general position (no two points have the same speed and no two points have the same x coordinate). The number of combinatorial changes in the Voronoi diagram of P over time is $O(n^2)$.

Proof. The proof uses linearization and follows Kol-tun's [8] proof. We parametrize a point $p_i(t) \in P$ as (x_i, tv_i) . The squared distance of any point (x, y) in the plane from $p_i(t)$ is

$$\begin{aligned} f_i^2(t, x, y) &= \text{dist}^2((x, y), p_i(t)) \\ &= (x - x_i)^2 + (y - tv_i)^2, \end{aligned}$$

$$f_i^2(t, x, y) = x^2 + y^2 + x_i^2 - 2x_i x - 2v_i y t + v_i^2 t^2.$$

Each vertex in the Voronoi diagram of the moving points corresponds to a vertex in the lower envelope of the family $\{f_i\}$. Let

$$g_i(t, x, y) = f_i^2(t, x, y) - x^2 - y^2.$$

Then the lower envelope of $\{f_i\}$ is combinatorially equivalent to that of $\{g_i\}$. Consider

$$g_i(t, x, y) = x_i^2 - 2x_i x - 2v_i y t + v_i^2 t^2.$$

Linearizing g_i , we take x, yt and t^2 as parameters in a 3-dimensional space, on which g_i is a linear function. The set $\{g_i\}$ is a set of 3-dimensional hyperplanes in the 4-dimensional space parametrized by x, yt and t^2 , and the complexity of its lower envelope is $O(n^2)$ [11]. This proves the desired upper bound. \square

2.3. The remaining 2 DOF cases

In this section, we derive bounds for other possible 2 DOF problems. In our scheme for measuring DOF, the general problem is represented by (x_0, y_0, v_x, v_y) and has 4 DOF. Since we can create a 2 DOF problem by choosing any two from our 4 DOF quadruple, there are six possible 2 DOF problems. We briefly discuss these six problems below.

$(x_0, y_0, 0, 0)$ —This is a static Voronoi diagram; each point in our set has only an initial position and 0 velocity. The complexity is $\Theta(n)$.

$(x_0, 0, v_x, 0)$ —In this case, each point is located on the x axis at time $t = 0$ and each point has its own constant velocity parallel to the x axis. Even in this very simple problem in which all the action takes place on a line, the complexity is $\Theta(n^2)$. To achieve the lower bound, we place a cluster of $n/2$ points on the x axis with velocity 0; the other $n/2$ points are placed in another cluster to the left of the first cluster. This second cluster has a velocity in the positive x direction. The points in the second cluster can be placed so that each point passes over each of the points in the first cluster causing $\Omega(n)$ changes in the Voronoi diagram. For a total of $\Omega(n^2)$. The upper bound of $O(n^2)$ can be shown by considering the point histories in the xt plane (i.e., graph each point's position as a function of time). Each point becomes a line in the xt

plane; changes in the Voronoi diagram correspond to line intersections. There are at most $O(n^2)$ such intersections.

$(x_0, 0, 0, v_y)$ —This is the case addressed in the preceding sections.

$(0, y_0, v_x, 0)$ —This is equivalent to case $(x_0, 0, 0, v_y)$.

$(0, y_0, 0, v_y)$ —This is equivalent to case $(x_0, 0, v_x, 0)$.

$(0, 0, v_x, v_y)$ —Each point has its own velocity, but each point starts at the origin. This case has complexity $\Theta(n)$ since at any given time the planar position of the points is the same as at time $t = \varepsilon$; only the scale is different.

Intuitively, we can draw the line between the linear complexity cases and the quadratic cases by using the *bypass* test. If one point can *bypass* another point then we are in quadratic territory.

In a very recent paper Koltun [8] comes up with yet another simplification of the Voronoi diagram of moving points. As in our setting the points here are on the x axis at time zero. But while in our setting the points move parallel to the y axis with various speeds, in his paper, the points are allowed to travel in any direction but all have the same constant speed. The resulting Voronoi diagram in his case is also of $\Theta(n^2)$ complexity. In our terms this is another case of a 2 DOF problem, in which one DOF is $v_{ix}^2 + v_{iy}^2$ equals a constant and the other DOF is the x_i coordinate at time zero. Another 2 DOF problem in this vein: all the points are on the same circle at time zero, and they all have a constant speed. In other words, for each point $v_{ix}^2 + v_{iy}^2 = C_1$ and $x_i^2 + y_i^2 = C_2$, where C_1 and C_2 are constants.

3. The related Minkowski sums

It has been shown [1] that, for the Minkowski sum corresponding to the Euclidean Voronoi diagram of lines in space, the combinatorial complexity has an upper bound of $O(n^{2+\varepsilon})$ and a lower bound of $\Omega(n^2)$. The same bounds also hold for the Minkowski sum corresponding to the Euclidean Voronoi diagram of points moving in the plane [1]. In this section we show that even for Minkowski sums corresponding to our simple 2 DOF Voronoi diagrams tight quadratic bounds are achieved.

3.1. Lower bound example

Given \mathcal{L} , a set of n lines in 3D, each parallel to the yz plane and intersecting the x axis, let \mathcal{D} be a unit disc parallel to the xy plane, and consider the complexity of $\mathcal{M} = \mathcal{L} \oplus \mathcal{D}$ (the Minkowski sum of \mathcal{L} and \mathcal{D}). This is the Minkowski sum problem corresponding to our 2 DOF $(x_0, 0, 0, v_y)$ planar Voronoi diagram problem with time represented as the z axis. We show that the combinatorial complexity of the boundary of \mathcal{M} is $\Omega(n^2)$.

Let $\ell \in \mathcal{L}$ be a line in 3D; we call $\ell \oplus \mathcal{D}$ a *pseudo cylinder*. In a standard cylinder the cross-section of the cylinder with a plane parallel to the xy plane is an ellipse and the cross-section with a plane perpendicular its line axis is a circle. For our pseudo cylinder the former is a circle and the latter is an ellipse.

Consider a set \mathcal{L} of n lines consisting of two disjoint subsets $\mathcal{L} = \mathcal{L}_1 \cup \mathcal{L}_2$. \mathcal{L}_1 is the set of $n/2$ lines which intersect the x axis at points $x_1, x_2, \dots, x_{n/2}$ within a segment of length ε where $\varepsilon \ll 1$ and $x_{i+1} - x_i = \varepsilon/n$. Each line ℓ_i in \mathcal{L}_1 has a straight line projection on the yz plane, describe by the line equation $y = v_i \cdot z$. Take $v_i < v_{i+1}$, for each $i < n/2$. \mathcal{L}_2 is the set of $n/2$ lines parallel to the z axis (with zero velocity) which intersect the x axis at points $x'_1, x'_2, \dots, x'_{n/2}$ in an interval of length δ , where $\delta < \varepsilon/n$, $x'_1 = 1 + x_{n/2} - \delta$ and $x'_{i+1} - x'_i = \delta/n$ (see Fig. 4).

Let $\mathcal{M}_1 = \mathcal{L}_1 \oplus \mathcal{D}$ and $\mathcal{M}_2 = \mathcal{L}_2 \oplus \mathcal{D}$. The boundary of \mathcal{M}_2 looks like a set of intersecting cylinders parallel to the z axis. A cross-section of \mathcal{M}_2 looks like the “mountain tops” in Fig. 3. \mathcal{M}_1 is a set of pseudo cylinders. The intersections of both \mathcal{M}_1 and \mathcal{M}_2 with the xy plane is shown in Fig. 4.

Consider the pseudo cylinders $c_i \in \mathcal{M}_1$ ($i = 1, \dots, n/2$), and a cylinder $c \in \mathcal{M}_2$. We claim that in our construction c intersects all the cylinders in \mathcal{M}_1 , causing $\Omega(n)$ intersection edges on the boundary of \mathcal{M} . Note that the cylinder c intersects the plane $y = 1$ in

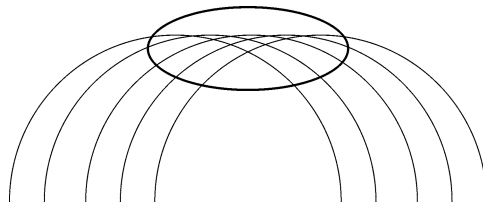
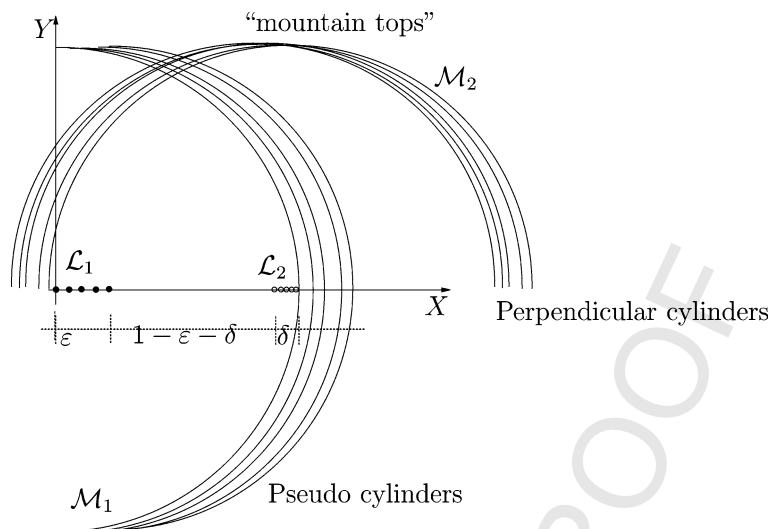


Fig. 3. Mountain tops.

Fig. 4. The intersections of \mathcal{L}_1 , \mathcal{L}_2 , \mathcal{M}_1 and \mathcal{M}_2 with the xy plane.

a line w parallel to the z axis. Since v_1 is $\min(v_i)$, for $i = 1, \dots, n/2$, the pseudo cylinder c_1 is the lowest pseudo cylinder of \mathcal{M}_1 to meet w on its boundary. We let w penetrate c_1 and exit from its higher side. The next slope v_2 is picked so that the mentioned exit point is on the boundary of \mathcal{M}_1 , and now w enters c_2 and so on, for all pseudo cylinders of \mathcal{M}_1 . In this construction w goes into and out of each pseudo cylinder of \mathcal{M}_1 and the entry/exit points are witnesses to the intersection edges of c and the corresponding pseudo cylinders of \mathcal{M}_1 . Since the cylinders in \mathcal{M}_2 are shifted by δ/n each such cylinder has a corresponding line w and thus performs the same entry/exit into cylinders of \mathcal{M}_1 , thus getting the $\Omega(n^2)$ complexity.

3.2. Upper bound proof

The complexity of the Minkowski sum of lines in space with a disc cannot be greater than the complexity of the corresponding Voronoi diagram [1], which was shown to be $O(n^2)$ in Section 2.2.

4. Lines in space with 2 DOF

For each problem involving moving points in the plane, there is a corresponding problem for lines in space. Our position and velocity quadruple (x_0, y_0, v_x, v_y) used for moving points in the plane becomes

a position and reciprocal-slope quadruple $(x_0, y_0, 1/m_{xz}, 1/m_{yz})$ for lines in space, where (x_0, y_0) represents where a line is allowed to intersect the $z = 0$ plane and where m_{xz} and m_{yz} are line slopes projected to the xz and yz planes, respectively.

Each of our constructions for the planar, moving-point problems has an analogous construction for 3D lines. The resulting upper and lower bounds are the same.

5. Future work

Sharp complexity bounds for the Voronoi diagram of moving points in the plane and for the Voronoi diagram of lines in space are clearly hard to achieve. Optimistically, we hope to inch toward sharp bounds for these general problems by solving next the 3 DOF problems followed by the full 4 DOF. There are four possible 3 DOF problems, but only two of these are really distinct. Sharp bounds for these two 3 DOF problems are, at present, unknown.

References

- [1] P.K. Agarwal, M. Sharir, Pipes, cigars and kreplach: the union of Minkowski sums in three dimensions, *Discrete Comput. Geom.* 24 (2000) 645–685.

49
50
51
52
53
54
55
56
57
58
59
60
61
62
63
64
65
66
67
68
69
70
71
72
73
74
75
76
77
78
79
80
81
82
83
84
85
86
87
88
89
90
91
92
93
94
95
96

- 1 [2] B. Aronov, A lower bound on Voronoi diagram complexity, 49
2 Inform. Process. Lett. 83 (4) (2002) 183–185. 50
- 3 [3] J.D. Boissonnat, M. Sharir, B. Tagansky, M. Yvinec, Voronoi 51
4 diagrams in higher dimensions under certain polyhedral dis- 52
5 tance functions, in: Proc. 11th ACM Symp. on Computational 53
6 Geometry, 1995, pp. 79–88. 54
- 7 [4] L.P. Chew, Near-quadratic bounds for the L_1 Voronoi diagram 55
8 of moving points, in: Proc. 5th Canad. Conf. Comput. Geom., 56
9 1993, pp. 364–369. 57
- 10 [5] L.P. Chew, K. Kedem, M. Sharir, B. Taganski, E. Welzl, 58
11 Voronoi diagrams of lines in 3-space under polyhedral convex 59
12 distance functions, J. Algorithms 29 (1998) 238–255. 60
- 13 [6] J.-J. Fu, R.C.T. Lee, Voronoi diagrams of moving points in the 61
14 plane, Internat. J. Comput. Geom. Appl. 1 (1991) 23–32. 62
- 15 [7] D.P. Huttenlocher, K. Kedem, J. Kleinberg, Voronoi diagrams 63
16 of rigidly moving sets of points, Inform. Process. Lett. 43 64
17 (1992) 217–223. 65
- 18 [8] V. Koltun, Ready, set, go!—The Voronoi diagram of moving 66
19 points that start from a line, Inform. Process. Lett. 89 (2004) 67
20 233–235. 68
- 21 [9] V. Koltun, M. Sharir, Three-dimensional Euclidean Voronoi 69
22 diagrams of lines with a fixed number of orientations, SIAM J. 70
23 Comput. 32 (2003) 616–642. 71
- 24 [10] L. Guibas, J.S.B. Mitchell, T. Roos, Voronoi diagrams of mov- 72
25 ing points in the plane, in: Proc. 17th Internat. Workshop 73
26 Graph-Theoret. Concepts Comput. Sci., in: Lecture Notes in 74
27 Comput. Sci., vol. 570, Springer-Verlag, Berlin, 1991, pp. 113– 75
28 125. 76
- 29 [11] R. Seidel, The upper bound theorem for polytopes: an easy 77
30 proof of its asymptotic version, Comput. Geom. Theory, 78
31 Appl. 5 (1995) 115–116. 79
32
33
34
35
36
37
38
39
40
41
42
43
44
45
46
47
48